

Extraterrestrial sound for planetaria: A pedagogical study

T. G. Leighton,^{a)} N. Banda, B. Berges, P. F. Joseph, and P. R. White

Institute of Sound and Vibration Research, University of Southampton, Highfield, Southampton SO17 1BJ, United Kingdom

(Received 31 January 2016; revised 10 July 2016; accepted 14 July 2016; published online 31 August 2016)

The purpose of this project was to supply an acoustical simulation device to a local planetarium for use in live shows aimed at engaging and inspiring children in science and engineering. The device plays audio simulations of estimates of the sounds produced by natural phenomena to accompany audio-visual presentations and live shows about Venus, Mars, and Titan. Amongst the simulated noise are the sounds of thunder, wind, and cryo-volcanoes. The device can also modify the speech of the presenter (or audience member) in accordance with the underlying physics to reproduce those vocalizations as if they had been produced on the world under discussion. Given that no time series recordings exist of sounds from other worlds, these sounds had to be simulated. The goal was to ensure that the audio simulations were delivered in time for a planetarium's launch show to enable the requested outreach to children. The exercise has also allowed an explanation of the science and engineering behind the creation of the sounds. This has been achieved for young children, and also for older students and undergraduates, who could then debate the limitations of that method.

© 2016 Acoustical Society of America. [<http://dx.doi.org/10.1121/1.4960785>]

[AGP]

Pages: 1469–1480

I. INTRODUCTION

Broadly speaking there are two roles that acoustics plays in astronomy. The first is the naturalization of time series from astronomical measurements that may or may not be acoustic. The second is the use of acoustics to study oscillatory mechanical waves in the type of extra-terrestrial bodies that can support them. These bodies include dust clouds, suns, etc., and this paper addresses sound in, or on, planetary bodies or moons. Collectively, these studies are sometimes referred to as “sound in space.” The naturalization process may involve transferring into audible signals previously non-acoustic time-series which occur in the vacuum or near-vacuum of space and which correspond to physical processes which do not represent pressure fluctuations. Their translation into an acoustic form is therefore entirely artificial, but useful as a means of experiencing the phenomenon in the familiar form of sound. One such example involves making audible recordings from the measured electromagnetic radiation signal from a pulsar.¹ The goal of such rendering is to facilitate a greater understanding of the data, or to make the data more accessible to the non-expert. Such approaches are based upon converting a time-series, which may derive from complex unfamiliar objects, into the familiar and information-rich medium of sound. Conversely, the study of the acoustics on extra-terrestrial bodies is concerned with considering the physical properties of an environment and sources, and predicting (and eventually interpreting) the character of sounds as they may appear on those bodies.

The synthesis of sounds from non-acoustic phenomena has been considered for a variety of astronomical

applications. Naturalization has been used to represent electromagnetic signals such as lightning on Jupiter or Saturn,² and the effect of a probe passing through the bow wave formed when solar emissions meet such a planet's massive magnetic field.³ It has also been used to create acoustic signals representing propagating density perturbations in dust clouds, nebulae, noctilucent clouds, planetary rings, comets, etc.^{4–9} Such low frequency, large scale perturbations, provide important information about the formation of stars and planets and their identification.^{10–14} Low frequency seismic and interface waves in stars and planetary bodies¹⁵ could also be auralized if converted to audible acoustic waves.

This paper considers problems which are a subset of the second category of sounds in space: the study of sounds on extra-terrestrial worlds. Work in this category can be further subdivided into two sub-classes. One is the prediction of the acoustical properties associated with physical processes that occur on the world under study. The other is the simulation of Earth-based sounds to recreate how they might be heard on another world. Predictions of the acoustic emissions from naturally occurring physical processes offers the possibility of designing systems that exploit these sounds to better understand the environment. Furthermore, these models can be used to test hypotheses on, for example, the nature of the natural sound sources; or the models could be used in an inverse mode to estimate the physical parameters of the source or environment from some future measurement of the acoustic signatures.

Understanding the acoustic environment on a planetary body allows the design of active acoustic instruments for use in probes or satellites. The most notable examples of this were associated with the highly successful Cassini-Huygens mission to Saturn's moon, Titan. Two acoustic instruments were

^{a)}Electronic mail: tgl@soton.ac.uk

developed for use on this mission. One was an acoustic altimeter,¹⁶ and another instrument used acoustic pulses transmitted between source and sensors on the probe to measure the atmospheric sound speed during descent.¹⁷ Future uses of sound range from the local (consideration of how the “ears” on a Martian space suit might better be able to warn an astronaut walking downhill of a rockfall behind him/her if the suit microphones are placed on the boot, not the helmet¹⁸) to the global (using the time taken for man-made or naturally occurring signals to propagate completely around the vast under-ice oceans of moons of Saturn and Jupiter to infer those ocean temperatures¹⁸).

The motivation of the work reported in this paper was to provide a method for simulating a range of audio signals of naturally occurring extra-terrestrial phenomena to engage the public in astronomy and related subjects. Simulating the acoustic environment on distant worlds is one way to capture the imagination of the broader community and can be used in conjunction with more conventional presentations. Indeed this project was the result of a requirement to augment an existing presentation in a local planetarium. An additional output was that simple physics lessons for public engagement and schools were developed. Two examples include the investigation of how everyday phenomenon would be transformed on others worlds, and (for the more engaged student) criticizing the limitations of the methods of producing those estimations. Acoustical phenomena are particularly useful for this purpose since humans have evolved to appreciate even the slightest nuances in sound, and because in some ways alien atmospheres can affect sound far more than, say, light, generating very significant and counterintuitive effects. With this in mind, this study sets out to provide a local planetarium with the ability to provide audiences with the estimates of acoustical phenomena from other worlds, supported by explanations that can be expressed in terms of school-level physics. Essential for those undertaking such tasks is an appreciation that the project plan must take account of low budgets and short time-scales.

For planetaria and film-makers, the current options of using Earth-based recordings of related phenomena, fictitious sounds or music, contrasts starkly with the integrity and detail available in the vast image libraries that can be readily accessed to portray planetary bodies.

In addition to public engagement and entertainment, there is another benefit to studying extra-terrestrial sound. It can reveal assumptions that have, over many years, been so well-validated from frequent application on Earth that they have become axiomatic. Testing them in extra-terrestrial environments can question that validation, improving instrument design and avoiding misinterpretations that can arise from the extra-terrestrial use of Earth-based intuition regarding sound and vibration. The use of common techniques for acoustic methods and definitions that are familiar practice on Earth can cause significant problems if applied to other worlds. Four examples are as follows:

- First, the fluid loading that is often taken for granted in Earth-based calibrations of sensors and tests can be significantly

different to that on Earth, depending on the geometry of the instrument and the atmosphere in which it is deployed;¹⁹

- Second, although measurements of the sound speed is an established method of determining some characteristics of atmospheric chemistry,²⁰ it has been found²¹ that an established design would work during Earth-based tests but be potentially misleading on Venus or the gas giants (for where it has been proposed^{20,22,23}).
- Third, in coming decades the acoustical exploration of the vast under-ice water oceans, which dwarf those on Earth, found in some moons of the gas and ice giants will be considered. To do so we will also be required revisit the basic physics instead of relying on Earth-based engineering intuition.¹⁸ For example, the hydrostatic pressure in these oceans will be the major factor in determining how acoustic rays refract, just as it does on Earth. However, in predicting such ray paths in extra-terrestrial oceans, the expression for hydrostatic pressure should not be the $\rho_w gh$ used by Earth ocean scientists and engineers (where ρ_w is the liquid density, g is the acceleration due to gravity, and h is the depth).^{24,25}
- Fourth, some terms in the sonar equations have become validated through decades of use in Earth’s oceans and the atmosphere within (at most) a few miles of the ground, but the nature of those terms might require re-examination if inaccuracies are to be avoided when applying them to extra-terrestrial scenarios.²⁶

The focus of this paper will be on sounds in the three substantial ground-level extra-terrestrial atmospheres in our solar system, namely, Venus, Mars, and Titan, the properties of which are found in Petculescu and Lueptow²⁷ and Leighton and White.²⁸ The planetarium show was designed to teach about sound by exploiting the audience’s familiarity with Earth-based sounds in air, comparing and contrasting these sounds with the extra-terrestrial ones. The audience would have had little experience with sounds in liquids and solids against which to benchmark the signals we produced for the planetarium, and therefore the choice was made to focus the effort on sounds in gases.

There are two types of prediction undertaken for this planetarium study: environmental sounds and the human voice. This paper focuses on some of the naturally occurring sounds that microphones of the future could potentially detect, focusing on thunder, dust devils and cryo-volcanoes. We simulated some of these sounds from the basic physics. However, in those cases where such simulations cannot even be made to produce a realistic Earth-like simulation of sound when Earth’s environmental parameters are used as input, then recordings of the equivalent sound on Earth are transmuted to adapt for the extra-terrestrial parameters. Therefore whilst the sound of thunder, dust devils, and a methanefall can be entirely simulated, the sound of cryo-volcanoes²⁹ is produced by transmuting a sound recorded on Earth (as is that of a Titan probe’s splashdown into a methane lake, though that is not detailed in this paper³⁰). This paper indicates where each simulation lies in the scale between a rigorous untested prediction, and a clip provided simply for entertainment in the absence of any competing clips.

Whilst the sound files produced for the above phenomena could conceivably be validated within the foreseeable future, the second type of prediction is entirely fictional, and that is the human voice. However, voice simulations are undertaken for two reasons. The first is to provide the planetarium with a way of engaging with the public, since the human ear is extremely well attuned to changes in the human voice, perhaps more than to any other sound. Moreover, the public is engaged simply because the speech on any of these worlds is unobtainable. The simulations undertaken here change the voice because of changes in sound speed and fluid loading, two separate effects that give rise to different anthropomorphic impressions (the size of the speaker and the pitch of the voice).^{31,32} In addition to entertainment, there is a further public engagement aspect of all these simulations. Most of the science stories in the media concern confirmed results, so that the public does not for the most part see the scenario in which scientists find themselves for most of their projects, between making a prediction from theory and waiting to see the extent to which measurements conflict with theory and require it to be amended, adapted, or replaced. The necessity of sending a probe to another world to make these observations produces a tangible barrier between the moment the prediction is published, and the point at which these simulations are tested against observation. This creates a sustained period in which the public, like the scientists, can criticize the approach and speculate on what must be done to increase the chances of making observations that are sufficiently good to discern the accurate predictions from the inaccurate.

II. BACKGROUND

A. Thunder

Terrestrial thunder is the pressure pulse produced when an atmospheric lightning charge causes a rapid expansion of atmospheric gas, initiated by the sudden outward thermal expansion (into the surrounding near-stationary cooler air) of the plasma in the lightning channel.³³ However, the character of the sound produced (a crack, a rumble, etc.) depends both on the shape of that electrical discharge (straight, forked, sheet, etc.) and features that affect propagation (ground and atmospheric characteristics, and range). The unrepresentative straight-line lightning channel assumed in the early simulations^{34,35} produced a single short thunder clap. Low frequency rumble was only added³⁶ when the channel geometry was made jagged.³⁷ In this paper, only the lightning between the atmosphere and ground is studied.

Atmospheric lightning on Venus is thought to occur at around half the rate seen on Earth. Its presence has been inferred from whistler-mode waves.³⁸ Although ground level wind velocities are low (1 m/s) in the hot (740 K), dense atmosphere (which has a ground level pressure of 9.3 MPa and density of 67 kg/m³, i.e., 6.5% that of liquid water on Earth),³⁹ at higher altitudes in Venus' complex atmosphere, windspeeds can exceed 100 m/s (6000% of the speed of planetary rotation, compared to ~20% seen for the fastest winds on Earth). The atmosphere is predominantly composed of carbon dioxide and the cloud content is dominated by sulphuric acid.

Mars does not have liquid-bearing clouds and so it does not have thunder storms, and therefore the lightning is assumed to occur because of the build-up of charge in dust devils. This thermally generated whirlwind, the lower part of which is made visible by the dust it raises, is a wholly separate phenomenon from a tornado. It is generated when solar heating of the ground causes hot air to rise up outside of the spinning column, while cooler air descends through its middle.⁴⁰ Charge distributions, like velocity profiles, are mutually dependent on the size and height of particles in the dust devil. Lightning is most likely from the larger dust devils (which tend to be less common than smaller ones), because the higher speeds within these can lift the heavier dust particles from the surface of Mars.⁴¹ All dust devils were found to have low frequency electromagnetic emissions, which may be used to detect their presence, location and velocity.⁴²

B. Dust devils

In addition to the possible generation of acoustic signals due to lightning, Martian dust devils would also generate pressure signals associated with pressure fluctuations due to convected turbulence. Measurements of the coherence function between closely spaced microphone signals would be useful to assess the relative contribution of acoustic and hydrodynamic signals, which tend to be coherent over much shorter distances than acoustic pressure fluctuations.

Solar radiation heats the ground, causing atmosphere near it to rise through the cooler air above it, which is at lower pressure. Thinning of the rising column causes mass to move toward the axis, generating strong spin through conservation of angular momentum, which is intensified as warmer ground-level air is drawn into the base of the dust devil.

One might consider designing acoustical detectors for probes, both for proximity warning and to open up the possibility of inversion of the emitted sound to measure dust devil parameters. To make such acoustical predictions, the mechanisms of sound production are quantitatively assessed using scaling laws derived by Morfe⁴³ to predict the sound power radiated to the far field, which are then corrected for atmospheric absorption. An energy spectrum is applied to this pressure field in order to obtain the frequency dependence. The resulting technique could predict the sound detected at a given range from a dust devil of a given size on Mars, having characteristics that change with the season and latitude.

C. Cryo-volcanoes

There is evidence suggesting the possible presence of cryo-volcanoes on Neptune's moon Triton, Jupiter's moons Io and Europa, and Saturn's moons Titan and Enceladus.⁴⁴⁻⁴⁶ Cryo-volcanoes may contribute to the high hydrocarbon content of Titan's atmosphere and surface,^{47,48} the hazy atmosphere of which would otherwise be depleted of hydrocarbon gases by sunlight through the photolysis that contributes to its characteristic haze and cloud cover. Unlike terrestrial volcanoes, which eject magma at high temperatures, cryo-volcanoes are cooler and release water, containing minerals, hydrocarbons (such as methane) and ammonia

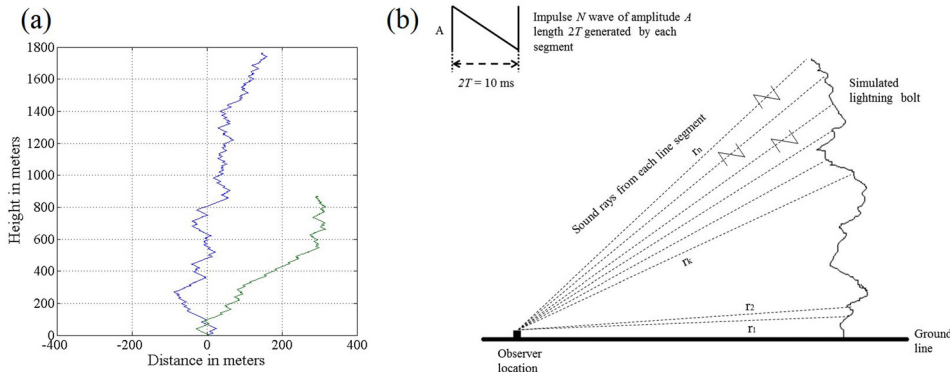


FIG. 1. (Color online) (a) Simulated lightning bolt generated using segment lengths of 2 m in random alignment, showing two different lightning strikes that impact the same point on the ground. (b) Thunder model as a linear superposition of N waves generated from lightning bolt segments.

(although on Titan the liquid content is probably dominated by hydrocarbons⁴⁹). The presence of liquid water in the moons of Saturn and Jupiter suggests heating by tidal forces, and in such circumstances pressurized water pockets can be generated and released to the surface (a solar heating model has also been proposed for Triton⁵⁰). In many ways, cryo-volcanoes/geysers on Titan resemble terrestrial geysers.⁴⁹

The objective in this paper is to provide details sufficient for schools to build their own model geysers or cryo-volcanoes and so stimulate discussion, rather than to duplicate any proposed mechanism by which a cryo-volcano might operate.

III. METHODS

The method by which the system for modifying speech is implemented has been described in detail previously.^{31,32} The methods for generating the sounds of methanefalls and splashdowns on Titan have also been detailed elsewhere.^{28,51} The sounds of voices and splashdowns used Earth-based recordings as their basis. The sounds of thunder, dust devils, and methanefalls were wholly simulated. The levels of rigor in deriving the sounds of dust devils and thunder were similar to those reported earlier for voices and methanefalls, commensurate with delivering only a first order study to produce a working device in short time scales. The sound of a cryo-volcano was less rigorous, being wholly contrived by building a physical model of a geyser. However, its inclusion was for a different purpose, specifically as follows:

- To provide details sufficient for a physical working model to be constructed from these schematics by schools themselves;
- To stimulate discussion of whether or not an atmosphere of some sort is needed in order to generate, propagate and detect sound in places other than our own planet.

A. Thunder

Following the method of Hill³⁷ for simulating realistic lightning paths with characteristic zig-zag profiles, spark sound sources were divided into line segments of given length and each segment was aligned at a random angle to the previous segment. The angles of inclination were selected from a random distribution (with a bias toward vertical axis to generate realistic shape of lightning bolt³⁶). Each line segment is then considered to be a source of sound. Using this

approach, various lightning profiles can be simulated, two of which are shown in Fig. 1(a) to strike the same point on the ground (which, in the case of Martian lightning, might be the lower intake zone of the dust devil). In this example, the longer lightning bolt is 1.8 km high and the shorter bolt is almost half its size at 850 m. The maximum size of the dust devils which might produce lightning bolts are believed to be 2 km to 8 km high. Figure 1 represents lightning bolts occurring in a medium-to-large dust devil with multiple electrical discharges.

In the absence of data on the lightning acoustic source strength on each planet, and because the atmospheric density and sound speed vary from site to site (making use of acoustic pressure problematic when comparing between planets²⁶), it was decided that each 2 m line segment would generate an N wave that had the same intensity 1 m from the centre of the segment (assuming spherical propagation). That intensity was 1 pW m^{-2} , chosen (i) to be small enough to ensure that acoustic pressure amplitudes do not become unfeasibly large in the thin Martian atmosphere, and (ii) for convenience, since the reference dB level for the lightning signals (perceived by an observer on the ground 1 km from the point where the lightning struck that ground) will be presented in dB relative to 1 pW m^{-2} (in compliance with international conventions⁵²). Consequently the outputs only serve to show the different absorbing features of the atmosphere, since only the absorbance and sound speed of the atmospheres (and the attenuation from spherical spreading, which is similar on all planets and so invisible when comparing them) affect the signal.²⁷ The N waves are modeled as initiating 1 m from the acoustic centre of the source,³⁷ rather than by nonlinear propagation in the atmosphere.⁵³ The signal at 1 km on flat ground from the point of strike was calculated, by assuming independent straight-line linear propagation path from each 2 m segment to the observer, through an atmosphere where the sound speed does not vary with height or frequency along the propagation path (Earth = 340 m/s; Venus = 410 m/s; Mars = 240 m/s; Titan = 210 m/s) and neither does the density [Earth = 1.2 kg/m^3 ; Venus = 65 kg/m^3 ; Mars = 0.02 kg/m^3 ; Titan = 5.5 kg/m^3 ; Fig. 1(b)]. The signals from the separate 2 m segments are linearly superimposed at the observer.³⁶

There are several important effects that are not included. The sound received at distance from the strike can be affected by the ground reflections, and the variation of atmospheric sound speed and absorption with frequency and

height.²⁷ Upwardly refracting atmospheres mean that sound emitted from the lightning channel above a certain height may not reach the observer on the ground. This can happen in cloud-to-cloud discharge when the lightning bolt is high in Earth's atmosphere. However, the low frequency acoustic components from cloud-to-ground discharges on Earth can usually be heard if the observer is less than 25 km away.³³ For Mars and Venus, Petculescu and Lueptow²⁷ observed that at the altitudes (below 8 km) and ranges (1–2 km) of interest, the sound speed over both the planets varies by only between 3 and 7 m/s, causing only small perturbations from straight-line propagation, and there is now increasing interest in the sound of lightning on Titan.^{54–56}

Even though Mars has a thin atmosphere, for the low altitudes under consideration here a continuum approach is assumed to hold.⁵⁷ The method does require that each N wave be represented as a pressure signal 1 m from the centre of its 2 m long source element, and obtaining the amplitude of this wave from the stated 1 pW m^{-2} intensity requires use of an assumed sound speed and atmospheric density for each planet. The method is made robust against details of the exact choice (because such exactitudes can be problematic²⁶) by ensuring that the reconstructed pressure time history at the observer is converted back to intensity using the same assumed sound speeds and densities. If we had not used the artifice that sound speed and density are constant along the propagation path, we would have opened up the question of what standard values to choose for each planet, and whether to convert using such a standard value or using the specific (and possibly different) values at range 1 m from the source and at the observer. The total acoustic pressure time series at the observer may be obtained by summing the pressures from the n th N wave segment of length l , assuming spherical spreading and including retarded time, as sketched in Fig. 1(b),

$$p(r, t) = A \int_{-l}^l \frac{N(ct - r_n)}{r_n} ds, \quad (1)$$

where c is the local speed of the sound, $N()$ is the time variation of the non-dimensional source strength of the waveform of the N wave, which has scaling amplitude A (in Pascals). The N wave has duration, $2T$, which relates to the energy released per unit length in the lightning discharge, and here is set to 10 ms. The lightning channel presented in Fig. 1(a) is used in Eq. (1) for the simulation of thunder noise on Venus, Mars, and Titan. Different realizations of the profile in Fig. 1(a) are computed, based on a random number generator to generate the angles between adjacent segments. The computations were performed to generate a signal at a sampling frequency of 44.1 kHz.

B. Dust devils

1. Sources in a dust devil

Noise from dust devils is likely to arise from three principal aerodynamic generation mechanisms: (i) infrasonic emissions, typically a few Hz, caused by low frequency oscillations of the entire rotating flow system;⁵⁸ (ii) the

generation of volumetric quadrupole sources arising from the fluctuating shear stress generated by turbulent mixing; (iii) sound generation by the acceleration of density inhomogeneities.

The dominant noise source mechanism (i) is inaudible and will not be considered here for a planetarium. Mechanism (ii) is associated with one of the highest scaling laws observed in nature. Following Lighthill,⁵⁹ the radiated noise power from turbulent mixing noise varies as the eighth power of mean flow speed. However, on both Earth and Mars, dust devil flows are restricted to low Mach numbers and this is not the dominant source of sound.

In this paper, we focus on the audible impression produced by mechanism (iii), although a future detector microphone might make significant use of (i). The sound produced by flow inhomogeneities at low flow speeds can be predicted to within an order of magnitude using the scaling laws.⁶⁰ That is to say, the density inhomogeneities of mass density ρ_s moving at a flow speed with mean velocity U distributed over a volume ΔV radiates at a distance r to a far field observer as

$$\overline{p^2} = \left(\frac{L}{r}\right)^2 \left(\frac{\rho_0 \rho_s}{c_0}\right)^2 U^6 \Delta V. \quad (2)$$

However, the above expression for overall mean square pressure provides no insight into the noise spectrum. For simplicity, we assume that

$$\overline{p^2}(f) = \overline{p^2} \Phi(f), \quad (3)$$

where $\Phi(f)$ is identical to the non-dimensional, normalized frequency spectrum for isotropic homogeneous turbulence with integral length scale L , given by

$$\Phi(f) = \frac{4}{U} \frac{L}{1 + (2\pi f L / U)^2}, \quad (4)$$

which has the normalization property

$$\int_0^\infty \Phi(f) df = 1. \quad (5)$$

The frequency spectrum of Eq. (5) has the characteristics of a low-pass filter with a cut-off frequency approximately equal to $(2\pi f L / U) = 1$. If we assume that the length-scale L scales with the dimensions of the dust devil itself then most of the noise is at very low frequencies, typically tens of Hz.

Overall noise from the dust devil can be predicted by summing the mean squared pressure from elementary volume contributions dV corresponding to regions between the ranges r and $r + dr$, the angles ϕ and $\phi + d\phi$ and height z and $z + dz$, and there $dV = dr r d\phi dz$ [Fig. 2(a)]. Finally, effects of atmospheric absorption on sound attenuation are added, following published theory.^{27,61–63}

The simple theory outlined above suggests that a simple prediction of the noise spectrum from a dust devil requires knowledge of the distribution of mean velocity, mass density, and turbulence length-scale throughout the volume of

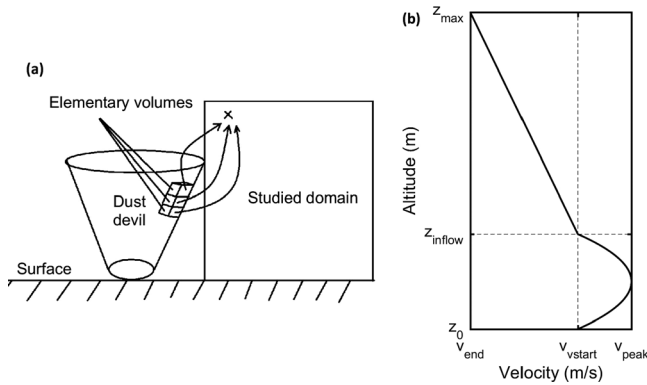


FIG. 2. (a) Sketch of the numerical model geometry for calculating the sound from the dust devil. (b) The scaling of flow velocity profiles (vertical, tangential, and radial) as a function of altitude for Martian dust devil calculations.

the dust devil. It was implemented assuming a ground-level sound speed somewhat further from the equator than that typical for the lightning of Sec. III A (220 m/s) and absorption as given by Petculescu and Lueptow.²⁷

A dust devil is characterized by three regions: the radial inflow region, the core region and the thermal plume region.⁶⁴ The radial inflow at the bottom of the dust devil corresponds to a very high vorticity region and the radial, tangential, and vertical velocities are higher in this region. This is represented by a quadratic increase and decrease with a peak at the middle of this region. Outside the inflow region, the velocity is defined by a slight linear decrease with altitude. This flow speed variation is illustrated in Fig. 2(b) showing the behavior of velocity components versus height z .

2. Calculation of input parameters

The mean flow speed variation in a typical dust devil was constructed from the literature,^{40,41,64} modeling the velocity profile in all three directions. Here we only summarize the main conclusions. The tangential velocity profile of dust devils approximates to a Rankine profile. In this, the tangential velocity in the main core of radius R_{core} is proportional to the radius, while the tangential velocity decreases as the inverse of the radius in the outer region of the vortex of radius R_{vortex} . The vertical velocity profile versus the radius has been predicted by numerical simulations of dust devils from large eddy simulations (LES) by Zhao *et al.*⁴⁰ It is characterized by an increase in velocity from the center to the end of the vortex core and then a decrease with distance. Finally, the horizontal profile of the radial velocity is described by Balme and Greeley⁴¹ and simulated by Zhao *et al.*⁴⁰ Both predictions indicate zero velocity inside the vortex core followed by an increase until a maximum value and then a decrease beyond that.

3. Density profile

The density profile required for the noise prediction is determined from the diameter of the particles inside the dust devil and the particle density. Following Jackson *et al.*,⁶⁵ a constant number density on the order of 10^8 grains/m³ was

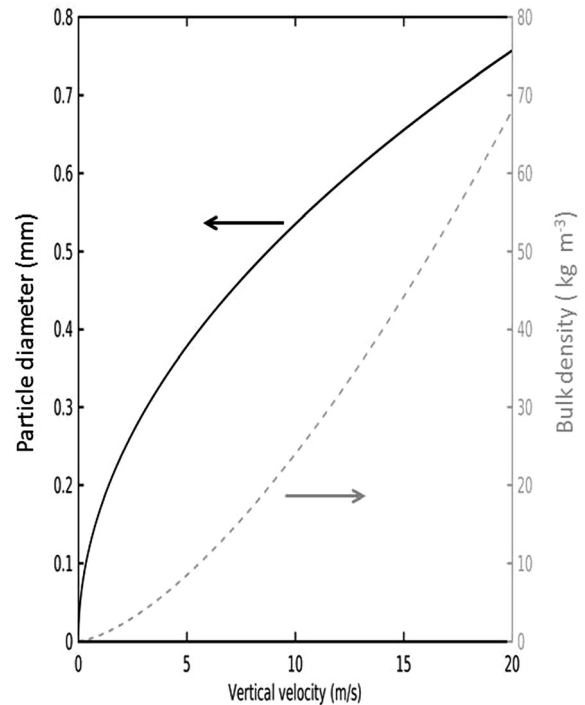


FIG. 3. The profiles, as a function of vertical lifting velocity, of the particle diameter (black, left) and bulk density (grey, right) profiles.

assumed for this simplified model of a Martian dust devil. The ability of the flow to lift dust and sand particles is related to the updraft speed of the dust devil. Grain diameters are calculated from the threshold “lifting” wind velocity⁶⁶ at which particles start moving in response to the action of the wind (each grain has a mineral density of 3000 kg m^{-3}). In the simulations here, the particle diameter and density profiles used are plotted as a function of the vertical speed in Fig. 3. The following representative values are assumed for the dust devil: the height of the dust devil $h = 250 \text{ m}$; the maximum radius of the core region of the dust devil $R_{\text{core}} = 50 \text{ m}$; the maximum radius of the vortex region of the dust devil $R_{\text{vortex}} = 70 \text{ m}$; the length scale of the dust devil $L = R_{\text{vortex}}/100$, used when defining the frequency dependence of the acoustic pressure field.⁶⁷ The initial, peak, and maximum mean velocities assumed in the simulations in the tangential direction v are (30, 35, 25) m/s, in the vertical direction w (20, 25, 15) m/s and in the radial direction u , (7, 5, 4) m/s, respectively.

C. Cryo-volcanoes

Figure 4 shows a schematic of the apparatus which models a terrestrial geyser [based on one built around 1977 by one of the authors (see Acknowledgements), and independently rediscovered more recently^{68,69}]. A flask of water (the “deep reservoir”) is continually heated, the only outlet being a long pipe that opens at the top to a “lake” (safely enclosed in the current version, but open to the lab in a “funnel” crater in the 1977 apparatus and in Lasic’s version⁶⁹). In the “lake” the water temperature is cooler. The following description enters the cycle just after an eruption, when cooler water from the lake has descended the tube into the deep reservoir.

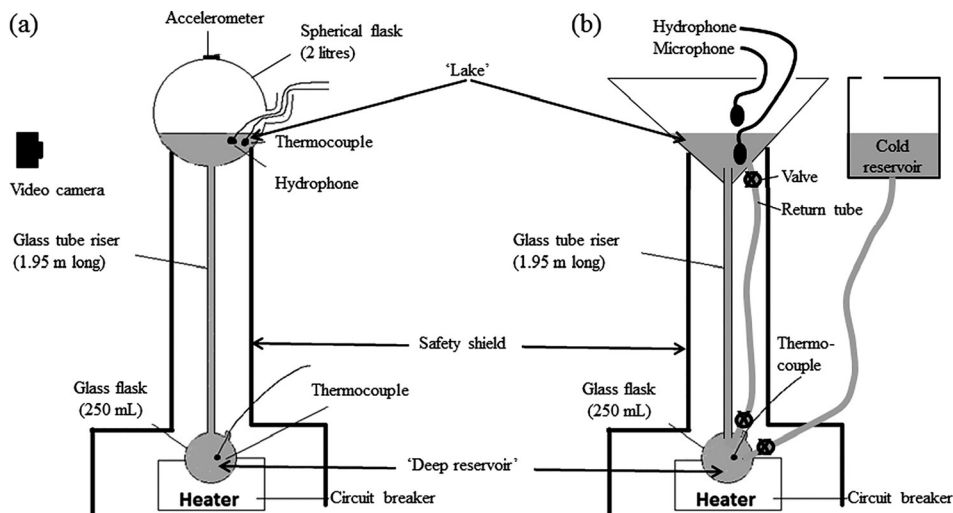


FIG. 4. Schematics of the two experimental arrangements used for the geyser/cryo-volcano.

As the temperature in the water at the base rises, gas comes out of solution: it had previously dissolved into the cooler lake water when it was open to the atmosphere (this of course invites discussion with undergraduates on how this apparatus compares to a cryo-volcano, and the role of static pressure and temperature, phase changes, and vapor).

Depending on the temperature and the static pressure (which may be very low close to the surface if there is no atmosphere) at key locations, boiling can occur. Water travels up the riser tube through a number of mechanisms: although thermal expansion does occur, level rise in the “lake” is dominated by the rise of any gas plugs and other bubbles up the pipe. This produces the gradual rise in lake level seen in terrestrial geysers before eruption. A key factor is the pressure in the deep reservoir, which sees a steady reduction if bubbles lift the water column above them, and also sees transient pressure changes as bubbles reach the lake prior to eruption: this can generate some splashing. Explosive eruption occurs because, whilst heat is being supplied to the base making it hotter, the pressure on the deep reservoir from the column of liquid is being reduced by the bubbles, lowering the boiling point in the flask. At a critical point, the rising temperature and reducing pressure pass a rapid transition to boiling phase, which causes mass and energy to travel from the deep reservoir to the lake. This persists until the eruption can no longer be sustained. Cooler water from the lake then travels down the riser tube to the deep reservoir (replenishing the reservoir with dissolved gas if the lake is open to the atmosphere), with commensurate condensation as cooling occurs, and the cycle begins again.

There is a layer of detail in the theory for the eruptions (including the roles of constrictions in the pipe, surface tension changes in the liquid, bubble traps etc.^{49,70,71}) that go into greater depth than this simple demonstration warrants (although limitations relating to the local sound speed, which are usually not important on Earth, have been proposed for other worlds⁴⁹). In this paper, two types of geyser will be produced, one that erupts at regular intervals, and one that does not erupt but delivers liquid and bubbles to the surface of the world or moon.

Figure 4 shows two versions of the apparatus that were built. Each contained 500 ml of water (when filled to generate

a “boiling” geyser—see Sec. III C), and a PMMA safety shield contains the apparatus. An electrical heater (Barnstead International 150 W, 2555 Kerper Boulevard Dubuque, Iowa, 52001-1478, USA) with a protective circuit breaker, was used. Depending on the availability of equipment, hydrophones (Bruel and Kjaer 8103, Herts, United Kingdom) and thermocouples were deployed in the lake and the deep reservoir, a microphone was set up in air by the lake (PCB ICP426E01, Piezotronics, Inc., NY), a video camera recorded the water level in the lake, and accelerometers (type 352C22) were placed on the flask containing the lake. Use of more sensors to map the signals at various locations and ranges was prevented by budget constraints, but would be desirable. Indeed, the use of a single microphone on a planetary probe does not allow identification of the source of pressure fluctuations on that microphone,⁷² i.e., whether they are truly acoustic (in that acoustical energy propagates to distance), or whether they are hydrodynamic or aerodynamic pressure fluctuations at source (or convected from some nearby source) that do not therefore represent the soundscape of that world, and should not be represented as such.

IV. RESULTS

A. Thunder

Figure 5 plots the intensity spectrograms recorded on flat ground 1 km from the point where lightning strikes the ground, with no refraction or ground effects included. Because each 2 m source segment emits an identical N wave of intensity 1 pW m^{-2} at 1 m from the acoustic centre of the element, the dB levels (re 1 pW m^{-2}) in Fig. 5 reflect the effects of atmospheric absorption.²⁷ Figure 5(a) shows the baseline, the thunder for the sound speed of Earth. The sound speed on Mars is low,²⁷ which would give a long detected signal except that the absorption on Mars is the highest of the planets studied here, and so does not allow the detected signal to persist [Fig. 5(b)]. Venus has the highest sound speed, so would have the shortest signal if no absorption were taken into account, although the received signal is dominated by the fact that at frequencies above around 100 Hz its absorption is substantially greater than that of

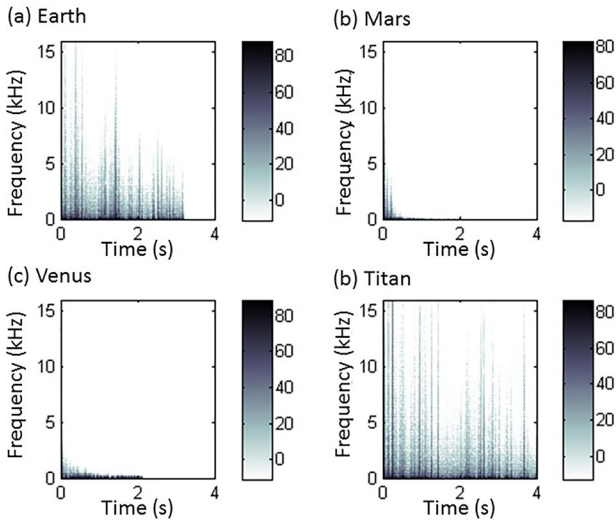


FIG. 5. (Color online) The greyscale plots the intensity on a time-frequency map for the predicted sound received on flat ground 1 km from the point where the lightning strike shown in Fig. 1 strikes the ground, for Earth, Mars, Venus, and Titan. No refraction or ground effects are included, and the artificial assumption is made that the lightning produces the same acoustic intensity at source, such that the dB levels (plotted re 1 pW m^{-2}) only reflect the effect of atmospheric absorption.

Earth's atmosphere.²⁷ Titan has, by a substantial margin, the lowest sound speed and absorption, so that its thunder signal persists the longest and contains significant high frequency information.

B. Dust devils

Figure 6 maps rms sound pressure level versus height and radial distance at four different frequencies: 500, 2000, 3500, and 5000 Hz. The sound pressure level decreases with frequency, range and height. The highest sound levels are

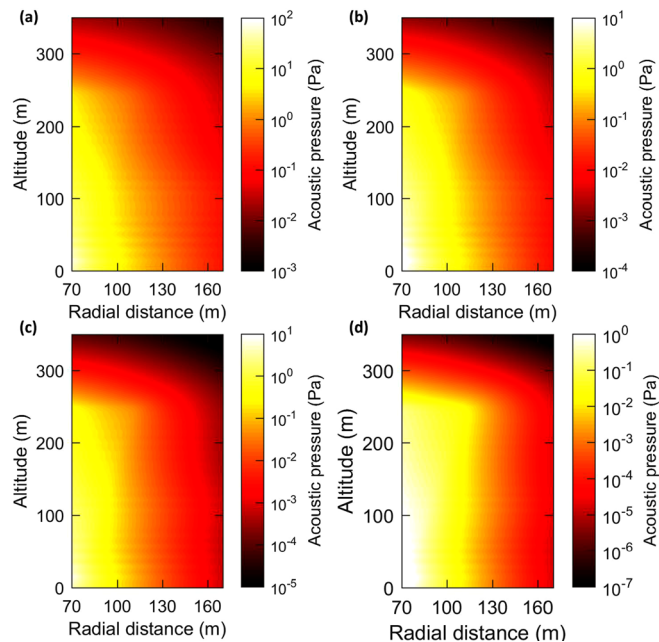


FIG. 6. (Color online) Simulated rms acoustic pressure from a Martian dust devil at (a) 500 Hz, (b) 2000 Hz, (c) 3500 Hz, and (d) 5000 Hz.

observed at locations closest to the inflow region of the dust devil, where the vorticity is highest. Although these predictions are subject to considerable uncertainties because the main parameters of density, length-scale, dust devil dimensions, and magnitude of the wind speed are themselves poorly understood in this scenario, nevertheless this simple approach provides a first order prediction of the noise spectra that is useful for illustrative purposes in the planetarium.

C. Cryo-volcanoes

With the apparatus shown in Fig. 4, a range of phenomena could be generated by, for example, allowing flow into the deep reservoir via the return tube and from the cold reservoir [items shown in (b) but not present in (a), these flows being controllable by valves]. The cold reservoir could be used to adjust the levels in the lake and provide different conditions or flow into the deep reservoir. The addition of anti-bumping granules to the deep reservoir ensured that the boiling of water would be uniform and not allow potentially unsafe superheated water to “shoot out.” However, from this range of possibilities, only two are reported in this paper: a “boiling” and an “overflowing/shooting” geyser. Other types of geyser (non-overflowing, pool, hot spring, and steam vent⁷³) were assessed as unsafe for use by students.

Preliminary experiments were conducted with the apparatus shown in Fig. 4(a). As the water temperature increases, previously dissolved gas comes out of solution, and small bubbles rise up the riser tube without significantly increasing the level of water in the lake. As the temperature increases, a rise in lake level [Fig. 7(a)] heralds violent boiling in the deep reservoir at a temperature of approximately 104°C , in agreement with calculations based on the extra static pressure contribution caused by the hydrostatic head of the riser tube and lake. When boiling occurs in the deep reservoir, a large vapor/gas bubble rises into the channel without collapsing, followed by other bubbles. When these bubbles reach the surface, a slight eruption starts. It lasts for a few seconds [from

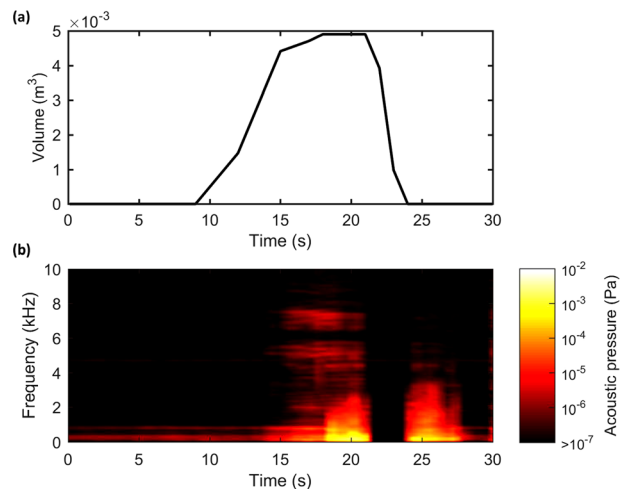


FIG. 7. (Color online) Simultaneous plots of (a) the change in volume in the upper lake during an eruption (the starting temperature at the lower reservoir was 80°C) and (b) the rms acoustic pressure record from a hydrophone in the lake in the upper flask (which at times was exposed to air – see text).

16 to 21 s in Fig. 7(b), as indicated by the record from a hydrophone placed 2 cm from the central axis of the upper flask] before there is insufficient pressure to prevent cooler water flowing back from the lake into the deep reservoir, such that the boiling stops. The drop of the water level in the upper flask is so great as to expose the hydrophone to air, so that it picks up no sound in the period 21–24 s. Use of a lake with deeper pockets would prevent this artifact.

Figure 8 shows the measurement over two eruptions of the temperature in the deep reservoir [Figs. 8(a) and 8(c)], and the lake [Figs. 8(b) and 8(d)], with two different lake starting temperatures, $\sim 50^\circ\text{C}$ [Figs. 8(a) and 8(b)] and $\sim 80^\circ\text{C}$ [Figs. 8(c) and 8(d)]. The data are averaged over 10 runs. The deep reservoir temperature oscillates in the expected manner, rising until eruption occurs, a process which is followed by cooling and condensation as cooler water flows from the lake to the deep reservoir. At lake temperatures below roughly 70°C , the lake temperature shows a gradual rise, on which are superimposed peaks during eruptions [Fig. 8(b)]. This trend ceases when the lake temperature reaches around 78°C , at which point the lake temperature oscillates around this value as eruptions heat it temporarily. A gradual rise in lake temperatures will tend to

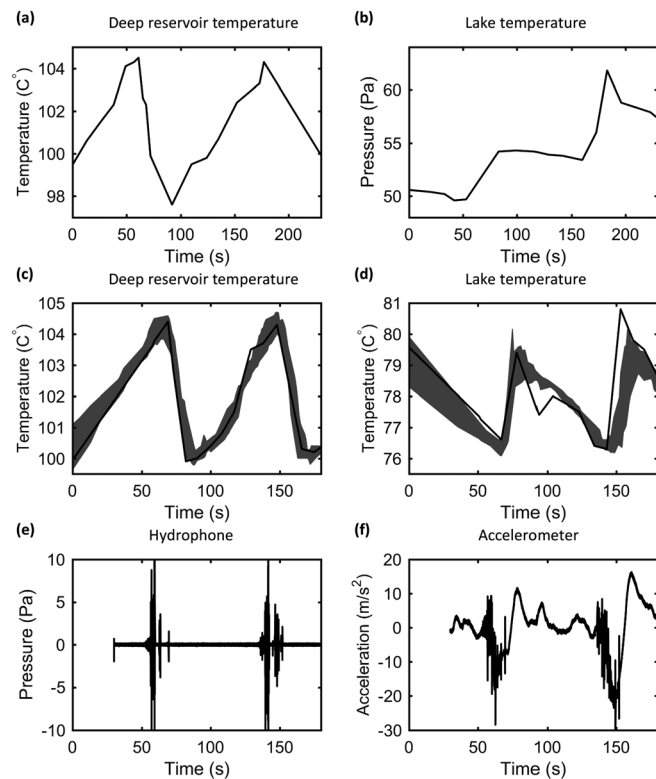


FIG. 8. Time histories of the temperature in [(a) and (c)] the deep reservoir and [(b) and (d)] the lake. (a) and (b) The first pair of simultaneous records are recorded when the lake temperature began at just over 50°C . (c) and (d) The second set of simultaneous data were recorded when the lake temperature oscillated around 78°C . Both were “boiling” eruptions. The black line in (c) and (d) is the temperature during one eruption cycle and the grey area represents the 25th–75th percentiles interval computed over ten consecutive eruption cycles. Concurrent with the black line temperature data in (c) and (d), panel (e) shows hydrophone data from the lake in the upper flask (note comments in Fig. 7), and panel (f) shows data from an accelerometer placed on the outside of the upper flask.

shorten the time between eruptions, as the deep reservoir requires less time to attain the temperature required to boil. The minimum in Fig. 8(a) is 97.5°C (and the time between eruptions is 125 s), several degrees cooler than the $\sim 100^\circ\text{C}$ minimum in Fig. 8(c), when there is only 80 s between eruptions.

Comparison of Figs. 8(c) and 8(d) most readily shows the steady state, where a steady temperature rise in the deep reservoir is followed by an eruption that warms the upper lake, after which water from the lake falls down the channel to cool the deep reservoir. A hydrophone in the lake [Fig. 8(e)] and an accelerometer on the outside of the upper flask [Fig. 8(f)], show eruption signals [the accelerometer not being prone to silence due to exposure in air which affects the hydrophone signal—see comments in caption to Fig. 7(a)]. While Fig. 7(a) showed that the lake level rises prior to the eruption as bubbles draw water up the riser tube, and returns to its original form after the eruption, the temperature sensors show that some water from the deep reservoir remains, raising its temperature [Figs. 8(b) and 8(d)] and some lake water falls to the deep reservoir, cooling it [Figs. 8(a) and 8(c)].

To generate time series suitable for use in our planetarium device, an in-air microphone was added outside the lake (3 cm from the water), a return feed was added from the lake to the deep reservoir, and the spherical container for the lake was replaced by a conical one. Unfortunately at this time the video camera, thermocouples and accelerometer were no longer available. A “boiling” geyser was generated by filling the upper flask (containing the lake) with water to a depth of 10 cm from the top of the riser tube. Once the cycle had been set up, it erupted every 356 s. A “shooting” or “overflowing” geyser was generated by keeping this flask mostly empty, the water being filled to the top of the riser tube only. Prior to an eruption, it rose by 10 mm, at which time the water temperature in the lake reached 102°C . Once in steady state, it erupted every 240 s, because of the volume and head of water were less than before.

The boiling geyser used the arrangement shown in Fig. 4(b), with the valves on the return tube open. When boiling is continuous in the deep reservoir, bubbles coalesce in the riser and are ejected only intermittently into the lake (with bubble sizes considerably larger than when they first enter the riser), which here is a reverberant environment (note that compared to free field, in a tube bubble dynamics will differ^{74–76}). With the same experimental arrangement, but with the lake flask empty in order to generate a shooting geyser, the microphone record is shown in Fig. 9(a). The microphone record is far more noisy than the hydrophone records of Figs. 7 and 8, largely because of the in-air sound in the laboratory. The electric heater at the deep reservoir was turned off at time $t=400$ s after the start of the recording, causing an almost immediate decrease in activity: whilst geothermal heat sources would not normally cease so suddenly, if intense differences in solar heating are a factor there will be such an effect, perhaps for example, in ice comets. The Welch Power Spectral Density estimate is shown in the inset, and indicates no signal above background above 3 kHz.

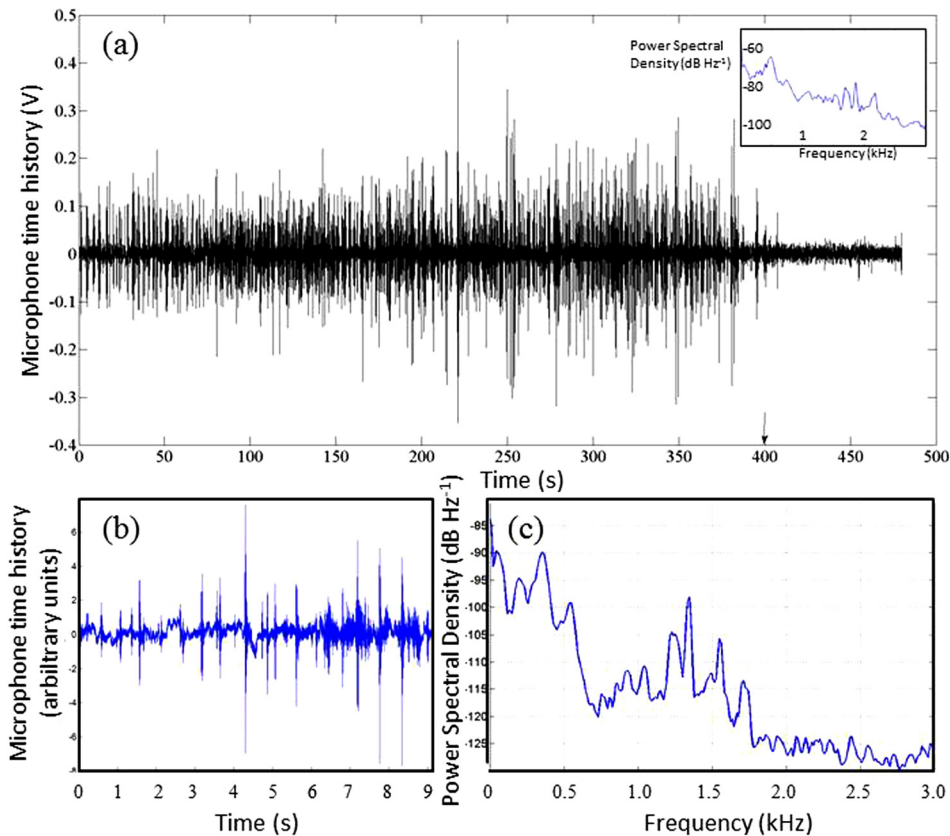


FIG. 9. (Color online) (a) Microphone data for in-air sound during a shooting eruption, with (inset) the Welch Power Spectral Density of the data. (b) and (c) Transposition of those data for Titan (arbitrary dB references are used for microphone voltages).

After testing both boiling and shooting geysers for the planetarium show,⁷⁷ the decision was made to use the in-air microphone recording of a shooting geyser as the basis for the planetarium show. This is because it served the purpose of requesting children in a show to imagine “what their ears might hear if they survived on Titan” than did the hydrophone record. It contained both the noise from the lake and the sound from the boiling deep reservoir.

For the purposes of the planetarium exhibition, a 9 s segment [Figs. 9(b) and 9(c)] was generated from the shooting geyser record of Fig. 9(a). There is currently too little information definitively to choose one method of transposing the geyser sounds from Earth to Titan. Previously,⁵¹ the Minnaert equation had been transposed from Earth to Titan to generate the sound of the “methanefall,” on the assumption that the natural frequencies of the bubbles would dominate the sound. Having used this method once,⁵¹ an alternative approach was chosen for the geyser, to open up discussions with undergraduates on their relative merits and validities and differing outcomes. For the geyser therefore, with little supporting evidence, the transposition was made as if the sound were dominated by the physical scale of the structures in air (transposing frequencies by the ratio of the ground level atmospheric sound speeds on the two worlds). The structures in question would include the lake craters, and the craters of popping bubbles. The latter was chosen because of its pedagogical potential: it celebrates the century since Sir William Bragg,⁷⁸ in the 1919 Royal Institution childrens’ Christmas lectures, suggested that the sounds emitted by running water originate from cavities created by the impact of liquid drops on the water surface. Bragg cited

the (previously unpublished) work of Sir Richard Paget who modeled these cavities (as photographed in 1908 by Worthington⁷⁹) out of plasticine and found that by blowing across openings in them sounds were produced similar to those heard when objects were dropped into water. Although replaced by the work of Minnaert as the established mechanism for bubble sounds, it was here (possibly erroneously) used to model a substantial contribution to the sounds of a Titan geyser.

V. PLANETARIUM FACILITY

The algorithms described in this paper were interfaced with a graphical user interface in a laptop and supplied to the Astrium Planetarium at INTECH, Winchester, UK (now Winchester Science Centre and Planetarium). Thunder on Mars, Venus, and Titan, dust devil noise on Venus, and the sound of cryo-volcanoes on Titan, were included using the methods of this paper. The device also included the sounds of methanefalls on Titan, a Titan probe’s splashdown into a methane lake, and a voice changer for Mars, Titan, and Venus, which have been described elsewhere.^{28,30,32,51} The first planetarium show featuring the device occurred on 4 April 2012.⁸⁰ Since then it also featured in the 19th Dutch Annual Quiz⁸¹ and in educational TV shows.⁸² Given the short timescales and lack of funding, the results have generated considerable interactions with the public, including formal presentations, Q&A sessions and school visits, etc. The validity of the simulations varies significantly, the assumptions and methods can readily be criticized and many could be improved upon. As such this work has facilitated considerable engagement with

undergraduate- and Masters-level students who have become interested in an area in which they can see their suggestions are capable of improving upon what is currently offered in this emerging area of research.

ACKNOWLEDGMENTS

The authors are grateful to Jenny Shipway and the staff of the Astrium Planetarium at INTECH, Winchester, UK. The authors are very grateful to Dr. Andi Petculescu for many fruitful discussions. T.G.L. is grateful to his physics teacher, Mr. Colin James of Heversham Grammar School, who in the 1970s constructed with him the first model geyser in order to test whether lake level rises preceded eruption, whether eruptions were associated with reduction in pressure as bubbles rose up the tube, and whether the timing between eruptions could be made regular and predictable. The data supporting this study, including time series, are openly available from the University of Southampton repository at <http://dx.doi.org/10.5258/SOTON/399196>.

¹Jodrell Bank Centre for Astrophysics, “The sounds of pulsars,” The University of Manchester <http://www.jb.man.ac.uk/pulsar/Education/Sounds/> (Last viewed January 31, 2016).
²Space Audio, “The sounds of lightning at Saturn,” The University of IOWA, <http://www-pw.physics.uiowa.edu/space-audio/cassini/cas-sed-06-023-2hr/> (Last viewed January 31, 2016).
³Space Audio, “Cassini encounters Saturn’s bow shock,” The University of IOWA, <http://cassini.physics.uiowa.edu/space-audio/cassini/bow-shock/> (Last viewed August 10, 2016).
⁴F. Verheest, “Are weak dust-acoustic double layers adequately described by modified Korteweg-de Vries equations?” *Phys. Scripta* **47**, 274–277 (1993).
⁵J. B. Pieper and J. Goree, “Dispersion of plasma dust acoustic waves in the strong-coupling regime,” *Phys. Rev. Letters* **77**, 3137–3140 (1996).
⁶M. Rosenberg and G. Kalman, “Dust acoustic waves in strongly coupled dusty plasmas,” *Phys. Rev. E* **56**, 7166–7173 (1997).
⁷R. L. Merlino, “Current-driven dust ion acoustic instability in a collisional dusty plasma,” *IEEE Trans. Plasma Sci.* **25**, 60–65 (1997).
⁸P. K. Shukla, “Dust acoustic wave in a thermal dusty plasma,” *Phys. Rev. E* **61**, 7249–7251 (2000).
⁹M. R. Gupta, S. Sarkar, S. Ghosh, M. Debnath, and M. Khan, “Effect of nonadiabaticity of dust charge variation on dust acoustic waves: Generation of dust acoustic shock waves,” *Phys. Rev. E* **63**, 046406 (2001).
¹⁰Y. Elsworth, R. Howe, G. R. Isaak, C. P. McLeod, and R. New, “Variation of low-order acoustic solar oscillations over the solar cycle,” *Nature* **345**, 322–324 (1990).
¹¹W. Rammacher and P. Ulmschneider, “Acoustic waves in the solar atmosphere. IX- Three minute pulsations driven by shock overtaking,” *Astron. Astrophys.* **253**, 586–600 (1992).
¹²U. Lee, “Acoustic oscillations of Jupiter,” *Astrophys. J.* **405**, 359–374 (1993).
¹³R. W. Noyes, S. Jha, S. G. Korzennik, M. Krockenberger, P. Nisenson, and T. M. Brown, “A planet orbiting the star ρ Coronae Borealis,” *Astrophys. J.* **483**, L111–L114 (1997).
¹⁴F. Bouchy, M. Bazot, N. C. Santos, S. Vaclair, and D. Sosnowska, “Asteroseismology of the planet-hosting star μ Arae. I. The acoustic spectrum,” *Astron. Astrophys.* **440**, 609–614 (2005).
¹⁵A. G. Kosovichev, “Properties of flares-generated seismic waves on the Sun,” *Sol. Phys.* **238**(1), 1–11 (2006).
¹⁶J. C. Zarnecki, M. R. Leese, B. Hathi, A. J. Ball, A. Hagermann, M. C. Towner, R. D. Lorenz, J. A. M. McDonnell, S. F. Green, M. R. Patel, T. J. Ringrose, P. D. Rosenberg, K. R. Atkinson, M. D. Paton, M. Banaszkiwicz, B. C. Clark, F. Ferri, M. Fulchignoni, N. A. L. Ghafoor, G. Kargl, H. Svedhem, J. Delderfield, M. Grande, D. J. Parker, P. G. Challenor, and J. E. Geake, “A soft solid surface on Titan as revealed by the Huygens Surface Science Package,” *Nature* **438**, 792–795 (2005).

¹⁷J. P. Lebreton, O. Witasse, C. Sollazzo, T. Blancquaert, P. Couzin, A.-M. Schipper, J. B. Jones, D. L. Matson, L. I. Gurvits, D. H. Atkinson, B. Kazeminejad, and M. Pérez-Ayúcar, “An overview of the descent and landing of the Huygens probe on Titan,” *Nature* **438**, 758–764 (2005).
¹⁸T. G. Leighton, P. R. White, and D. C. Finfer, “The opportunities and challenges in the use of extra-terrestrial acoustics in the exploration of the oceans of icy planetary bodies,” *Earth Moon Planets* **109**(1-4), 91–116 (2012).
¹⁹T. G. Leighton, “Fluid loading effects for acoustical sensors in the atmospheres of Mars, Venus, Titan and Jupiter,” *J. Acoust. Soc. Am.* **125**(5), EL214–EL219 (2009).
²⁰R. A. Hanel, “Exploration of the atmosphere of Venus by a simple capsule,” NASA Technical Note TN D-1909 (1964).
²¹J. Jiang, K. Baik, and T. G. Leighton, “Acoustic attenuation, phase and group velocities in liquid-filled pipes II: Simulation for spallation neutron sources and planetary exploration,” *J. Acoust. Soc. Am.* **130**(2), 695–706 (2011).
²²R. A. Hanel and M. G. Strange, “Acoustic experiment to determine the composition of an unknown planetary atmosphere,” *J. Acoust. Soc. Am.* **40**, 896–905 (1966).
²³D. Banfield, P. Gierasch, and R. Dissly, “Planetary descent probes: Polarization nephelometer and hydrogen ortho/para instruments,” *Proc. IEEE Aerosp. Conf.* **2005**, 691–697.
²⁴T. G. Leighton, D. C. Finfer, and P. R. White, “The problems with acoustics on a small planet,” *Icarus* **193**(2), 649–652 (2008).
²⁵T. G. Leighton, “The use of extra-terrestrial oceans to test ocean acoustics students,” *J. Acoust. Soc. Am.* **131**(3 Pt 2), 2551–2555 (2012).
²⁶M. A. Ainslie and T. G. Leighton, “Sonar equations for planetary exploration,” *J. Acoust. Soc. Am.* **140**, xxx (2016).
²⁷A. Petculescu and R. M. Lueptow, “Atmospheric acoustics of Titan, Mars, Venus, and Earth,” *Icarus* **186**, 413–419 (2007).
²⁸T. G. Leighton and P. R. White, “The sound of Titan: A role for acoustics in space exploration,” *Acoust. Bull.* **29**(4), 16–23 (2004).
²⁹J.-R. Cook, D. C. Brown, and P. Laustsen, “Cassini spots potential ice volcano on Saturn moon,” Cassini Solstice Mission, News and Features (December 14, 2010), Jet Propulsion Laboratory California Institute of Technology, <http://saturn.jpl.nasa.gov/news/newsreleases/newsrelease20101214/> (Last viewed December 5, 2015).
³⁰T. G. Leighton and P. R. White, “The sounds of voices and waterfalls on other planets,” http://www.southampton.ac.uk/engineering/research/projects/the_sounds_of_voices_and_waterfalls_on_other_planets.page (Last viewed June 23, 2016).
³¹T. G. Leighton and A. Petculescu, “The sound of music and voices in space Part 1: Theory,” *Acoust. Today* **5**(3), 17–26 (2009).
³²T. G. Leighton and A. Petculescu, “The sound of music and voices in space Part 2: Modeling and simulation,” *Acoust. Today* **5**(3), 27–29 (2009).
³³V. A. Rakov and M. A. Uman, *Lightning: Physics and Effects* (Cambridge University Press, Cambridge, UK, 2007), 687 pp.
³⁴M. N. Plooster, “Numerical model of the return stroke of the lightning discharge,” *Phys. Fluids* **14**, 2124–2133 (1971).
³⁵R. D. Hill, “Channel heating in return-stroke lightning,” *J. Geophys. Res.* **76**, 637–645, doi:10.1029/JC076i003p00637 (1971).
³⁶H. S. Ribner and D. Roy, “Acoustics of thunder: A quasilinear model for tortuous lightning,” *J. Acoust. Soc. Am.* **72**(6), 1911–1925 (1982).
³⁷R. D. Hill, “Analysis of irregular paths of lightning channels,” *J. Geophys. Res.* **73**(6), 1897–1906, doi:10.1029/JB073i006p01897 (1968).
³⁸C. T. Russell, T. L. Zhang, M. Delva, W. Magnes, R. J. Strangeway, and H. Y. Wei, “Lightning on Venus inferred from whistler-mode waves in the ionosphere,” *Nature* **450**(7170), 661–662 (2007).
³⁹A. T. Basilevsky and J. W. Head, “The surface of Venus,” *Rep. Prog. Phys.* **66**(10), 1699–1734 (2003).
⁴⁰Y. Z. Zhao, Z. I. Gu, Y. Z. Yu, Y. Ge, Y. Li, and X. Feng, “Mechanism and large eddy simulation of dust devils,” *Atmos. Ocean* **42**(1), 61–84 (2004).
⁴¹M. Balme and R. Greeley, “Dust devils on Earth and Mars,” *Rev. Geophys.* **44**(3), RG3003, doi:10.1029/2005RG000188 (2006).
⁴²N. O. Renno, A.-S. Wong, and S. K. Atreya, “Electrical discharges and broadband radio emission by Martian dust devils and dust storms,” *Geophys. Res. Lett.* **30**(22), 2140, doi:10.1029/2003GL017879 (2003).
⁴³C. L. Morfey, “Amplification of aerodynamic noise by convected flow inhomogeneities,” *J. Sound Vib.* **31**(4), 391–397 (1973).
⁴⁴J. R. Spencer, J. C. Pearl, M. Segura, F. M. Flasar, A. Mamoutkine, P. Romani, B. J. Buratti, A. R. Hendrix, L. J. Spilker, and R. M. C. Lopes, “Cassini encounters Enceladus: Background and the discovery of a south polar hot spot,” *Science* **311**, 1401–1405 (2006).

- ⁴⁵C. C. Porco, P. Helfenstein, P. C. Thomas, A. P. Ingersoll, J. Wisdom, R. West, G. Neukum, T. Denk, R. Wagner, T. Roatsch, S. Kie_er, E. Turtle, A. McEwen, T. V. Johnson, J. Rathbun, J. Veverka, D. Wilson, J. Perry, J. Spitalo, A. Brahic, J. A. Burns, A. D. DelGenio, L. Dones, C. D. Murray, and S. Squyres, "Cassini observes the active south pole of Enceladus," *Science* **311**, 1393–1401 (2006).
- ⁴⁶S. Bargmann, R. Greve, and P. Steinmann, "Simulation of cryo-volcanism on Saturn's Moon Enceladus with the Green-Naghdi theory of thermo-elasticity," *Bull. Glaciol. Res.* **26**, 23–32 (2008).
- ⁴⁷C. Sotin, R. Jaumann, B. J. Buratti, R. H. Brown, R. N. Clark, L. A. Soderblom, K. H. Baines, G. Bellucci, J.-P. Bibring, F. Capaccioni, P. Cerroni, M. Combes, A. Coradini, D. P. Cruikshank, P. Drossart, V. Formisano, Y. Langevin, D. L. Matson, T. B. McCord, R. M. Nelson, P. D. Nicholson, B. Sicardy, S. Lemouelic, S. Rodriguez, K. Stephan, and C. K. Scholz, "Release of volatiles from a possible cryovolcano from near-infrared imaging of Titan," *Nature* **435**(7043) 786–789 (2005).
- ⁴⁸A. Coustenis and M. Hirtzig, "Cassini-Huygens results on Titans surface," *Res. Astron. Astrophys.* **9**(3), 249–268 (2009).
- ⁴⁹R. D. Lorenz, "Thermodynamics of geysers: Application to Titan," *Icarus* **156**, 176–183 (2002).
- ⁵⁰R. L. Kirk, L. A. Soderblom, and R. H. Brown, "Subsurface energy storage and transport for solar-powered geysers on Triton," *Science* **250**, 424–429 (1990).
- ⁵¹T. G. Leighton, P. R. White, and D. C. Finfer, "The sounds of seas in space," in *Proceedings of the International Conference on Underwater Acoustic Measurements, Technologies and Results*, Heraklion, Crete (June 28 to July 1, 2005), 833–840.
- ⁵²ISO 1683:2015: *Acoustics – Preferred Reference Values for Acoustical and Vibratory Levels* (International Organization for Standardization, Geneva, Switzerland, 2015).
- ⁵³T. G. Leighton, "What is ultrasound?" *Prog. Biophys. Mol. Biol.* **93**(1–3), 383 (2007).
- ⁵⁴A. Petculescu, "A tool to corroborate lightning and a first step toward a Titanian sound scape," <http://acoustics.org/pressroom/httpdocs/159th/petculescu.htm> (Last viewed January 10, 2016).
- ⁵⁵A. Petculescu and P. Achi, "A model for the vertical sound speed and absorption profiles in Titan's atmosphere based on Cassini-Huygens data," *J. Acoust. Soc. Am.* **131**, 3671–3679 (2012).
- ⁵⁶C. S. Hill and A. Petculescu, "Gasdynamic modeling of strong shock wave generation from lightning in Titan's troposphere," *J. Acoust. Soc. Am.* **129**, 2411 (2011).
- ⁵⁷A. D. Hanford and L. N. Long, "The direct simulation of acoustics on Earth, Mars and Titan," *J. Acoust. Soc. Am.* **125**(2), 640–650 (2009).
- ⁵⁸A. J. Abdullah, "The 'musical' sound emitted by a tornado," *Mon. Weather Rev.* **94**(4), 213–220 (1966).
- ⁵⁹M. J. Lighthill, "On sound generated aerodynamically. I. General theory," *Proc. R. Soc. Lond. A* **222**, 564–587 (1952).
- ⁶⁰C. L. Morfey, "Amplification of aerodynamic noise by convected flow inhomogeneities," *J. Sound Vib.* **31**, 391–397 (1973).
- ⁶¹H. E. Bass and J. P. Chambers, "Absorption of sound in Martian atmosphere," *J. Acoust. Soc. Am.* **109**(6), 3069–3071 (2001).
- ⁶²J.-P. Williams, "Acoustic environment of the Martian surface," *J. Geophys. Res.* **106**(E3), 5033–5041, doi:10.1029/1999JE001174 (2001).
- ⁶³Y. Drain and R. M. Lueptow, "Acoustic attenuation in three-component gas mixtures – Theory," *J. Acoust. Soc. Am.* **109**, 1955–1964 (2001).
- ⁶⁴T. J. Ringrose, M. R. Patel, M. C. Towner, M. Balme, S. M. Metzger, and J. C. Zarnecki, "The meteorological signatures of dust devils on Mars," *Planet. Space Sci.* **55**, 2151–2163 (2007).
- ⁶⁵T. L. Jackson, W. M. Farrell, G. T. Delory, and J. Nithianandam, "Martian dust devil electron avalanche process and associated electrochemistry," *J. Geophys. Res.* **115**, E05006, doi:10.1029/2009JE003396 (2010).
- ⁶⁶Z. Gu, Y. Zhao, Y. Li, Y. Yu, and X. Feng, "Numerical simulation of dust lifting within dust devils - simulation of an intense vortex," *J. Atmos. Sci.* **63**, 2630–2641 (2006).
- ⁶⁷J. O. Hinze, *Turbulence, McGraw-Hill Series in Mechanical Engineering* (McGraw-Hill, New York, 1975).
- ⁶⁸N. Saptadji and D. H. Freeston., "Laboratory model of geysers: Some preliminary results," in *Proceedings 13th Zealand Geothermal Workshop* (1991), pp. 155–160.
- ⁶⁹S. Lasic, "Geyser model with real-time data collection," *Eur. J. Phys.* **27**, 995–1005 (2006).
- ⁷⁰X. Lu and A. Watson, "A review of progress in understanding geysers," in *Proceedings World Geothermal Congress 2005*, Antalya, Turkey (April 24–29, 2005), 6 pp.
- ⁷¹E. Adelstein, A. Tran, C. Muñoz Saez, A. Shteinberg, and M. Manga, "Geyser preplay and eruption in a laboratory model with a bubble trap," *J. Volcanol. Geotherm. Res.* **285**, 129–135 (2014).
- ⁷²B. Berges, "The creation of extraterrestrial soundscapes by simulating the sounds of other worlds," M.Sc. thesis, University of Southampton, Southampton, UK, 2011, 99 pp.
- ⁷³N. M. Saptadji, "Modeling of geysers," Ph.D. thesis, Department of Engineering Science, School of Engineering, University of Auckland, Auckland, New Zealand, 1995, 403 pp.
- ⁷⁴T. G. Leighton, P. R. White, and M. A. Marsden, "The one-dimensional bubble: An unusual oscillator, with applications to human bioeffects of underwater sound," *Eur. J. Phys.* **16**, 275–281 (1995).
- ⁷⁵T. G. Leighton, P. R. White, and M. A. Marsden, "Applications of one-dimensional bubbles to lithotripsy, and to diver response to low frequency sound," *Acta Acust.* **3**(6), 517–529 (1995).
- ⁷⁶T. G. Leighton, "The inertial terms in equations of motion for bubbles in tubular vessels or between plates," *J. Acoust. Soc. Am.* **130**(5), 3333–3338 (2011).
- ⁷⁷M. N. Banda, "Acoustics of natural phenomena on other planets and satellites," M.Sc. thesis, University of Southampton, Southampton, UK, 2011, 93 pp.
- ⁷⁸W. H. Bragg, *The World of Sound* (G. Bell and Sons Ltd., London, UK, 1921), 196 pp.
- ⁷⁹A. M. Worthington, *A Study of Splashes* (Longmans, Green, and Company, London, UK, 1908), 129 pp.
- ⁸⁰University of Southampton, "The world's first planetarium show featuring the sounds and voices of other worlds," http://www.southampton.ac.uk/engineering/research/projects/media/sound_in_space/worlds_first_planetarium_show.page (Last viewed January 31, 2016).
- ⁸¹University of Southampton, "Southampton software used in the 19th Dutch Annual Quiz," http://www.southampton.ac.uk/engineering/research/projects/media/sound_in_space/19th_dutch_annual_quiz.page (Last viewed January 31, 2016).
- ⁸²University of Southampton, "BBC's The Sky At Night features voice changer," http://www.southampton.ac.uk/engineering/research/projects/media/sound_in_space/bbc_the_sky_at_night.page (Last viewed January 31, 2016).